CRYSTAL GROWTH & DESIGN
2009
VOL. 9, NO. 7
3260–3264

Growth and Investigation of Crystals of the New Superconductor α-FeSe from KCl Solutions

B. H. Mok,*,† S. M. Rao,*,‡ M. C. Ling,‡ K. J. Wang,‡ C. T. Ke,‡ P. M. Wu,§ C. L. Chen,‡ F. C. Hsu,†,‡ T. W. Huang,‡ J. Y. Luo,‡ D. C. Yan,‡ K. W. Ye,‡ T. B. Wu,† A. M. Chang,§ and M. K. Wu†,‡

Institute of Physics, Academia Sinica, Nankang, Taipei, Taiwan, Department of Materials Science and Engineering, National Tsing Hua University, Hsinchu, Taiwan, and Department of Physics, Duke University, Durham, NC 27708

Received December 31, 2008; Revised Manuscript Received March 23, 2009

ABSTRACT: Crystals of $FeSe_{0.88}$ and $FeSeMn_{0.1}$ have been grown from KCl solutions. Crystals measuring 2−3 mm across and 0.1−0.3 mm thick grow with a hexagonal plate like habit. Powder X-ray diffraction (XRD) measurements show strong peaks corresponding to the tetragonal α-FeSe phase and weak hexagonal β-FeSe peaks in both cases. The plate side of the crystal is identified to be the (101) face of the tetragonal α-FeSe. Energy dispersive X-ray spectroscopic (EDS) measurements show that Mn substitutes for Fe. Both types of crystals show a superconducting transition at 8 K in the DC magnetization measurements and a broad resistive transition with zero resistance at 7.5 K with an onset at 11 K. Specific heat measurements also confirm bulk superconductivity in the crystals. Crystals could also be grown using KBr as a solvent.

1. Introduction

α-FeSe is a well-investigated room temperature ferromagnetic material[1−6] that is found to exhibit superconductivity at 8 K with a slight deficiency of Se.[7] The superconductivity in FeSe came to light following the discovery of superconductivity at 26 K in $LaFeAs(O_{1-x}F_x)$.[8,9] Investigations on the less toxic FeSe started in our laboratory following these earlier reports. It was found that the α-FeSe phase is responsible for superconductivity. This phase could be stabilized by preparing the bulk samples with a slight deficiency of Se and annealing them at 400 °C for a long time (∼15−20 h). In a short time several reports covering both experimental and theoretical aspects have appeared on FeSe[10−16] including one of an increase of T_c to 27 K under high pressure.[12] Even though preparations of thin films of tetragonal FeSe have been reported in the past[5,6] (for magnetic applications), the growth of single crystals of the superconductor only appeared very recently.[10] Since single crystals are important to obtain the correct phase devoid of impurity phases[7] and to understand underlying mechanisms, we undertook the growth of crystals of FeSe soon after the discovery of superconductivity in this system. FeSe is known to melt congruently around 1075 °C from the phase diagram reported in the literature.[4] However, the high vapor pressure of Se at this temperature would impede the growth of the α-FeSe phase deficient in Se by the melt growth techniques.[2] We therefore tried growing the crystals by some of the low temperature methods such as hydrothermal, vapor transport and high temperature solution growth. The efforts to grow crystals by the high temperature solution growth technique[17] yielded good results, using KCl or KBr as a solvent. Stable α-FeSe crystals with hexagonal plate like morphology were obtained with both solvents. The growth details and properties of the crystals grown in KCl solutions are reported here.

2. Experimental Section

Crystals were grown in a homemade vertical wire wound tube furnace. A Yokagawa UP550 Programmer coupled to a suitable power supply was used to control the temperature in the furnace with an accuracy of ±0.3 °C. The powder X-ray diffraction measurements were made on a Phillips PW3040/60 diffractometer using Cu Kα radiation and a Ni filter. Magnetic measurements were made using a Quantum Design Magnetic Property Measurement System (MPMS) and the resistivity measurements in a Physical Property Measurement System (PPMS) of the same make.

To obtain the tetragonal α-FeSe[7] phase, initially we attempted growing the crystals under high pressure by the hydrothermal growth technique with the hope that lower temperature (220−300 °C) and high pressure would stabilize the α-phase. Large crystals with octahedral faces measuring nearly 2−3 mm were obtained (not presented here). These crystals quickly broke down to microscopic crystallites of FeSe, FeO complexes on exposure to atmospheric pressure and did not represent stable α-FeSe. Vapor transport technique using iodine and bromine as carriers was also tried for growing crystals with some success but will not be discussed here.

To grow crystals from high temperature solutions, prereacted powders of $FeSe_{0.88}$ and $FeSe:Mn_{0.1}$ were loaded into quartz crucibles along with KCl. A KCl to FeSe ratio of 10:1 was maintained. The solubility of FeSe in KCl was obtained by melting KCl mixed with different amounts of FeSe in small evacuated quartz crucibles and rapidly cooling them. It was found that the addition of stoichiometric proportions of Fe and Se also produced crystals as good as the prereacted powders. Therefore in the later experiments prereacted powders were not used. All the powders were stored in dryboxes to prevent oxidation due to atmospheric contact. KCl and KBr powders were heated to 450 °C before filling into the quartz crucibles to remove traces of moisture that might be present from causing oxidation of the crystals during growth. The quartz crucibles were sealed in a vacuum better than 1×10^{-4} mbar. Three to four crucibles of 8 mm inner diameter were placed together in an alumina crucible filled with alumina powder to provide additional thermal mass and temperature stability. Larger diameter tubes were used to obtain bigger crystals. The temperature of the crucibles was monitored using a separate thermocouple placed in the alumina powder. The temperature of the furnace was raised to 840 °C and held for 30 h to homogenize the solution. It was cooled to 820 °C in 1 h to provide the necessary supersaturation for nucleation. Further cooling was programmed at 0.3−0.5 °C/h from 820 to 770 °C. Then the furnace was rapidly cooled to 400 °C and held for 24 h as this helps in stabilizing the α-FeSe phase.[7] This was followed by rapid cooling to room temperature in 2−3 h. After the furnace cooled to room temperature, the crucible was taken out of the

* Corresponding authors. E-mail: rao@phys.sinica.edu.tw (S.M.R); d937536@oz.nthu.edu.tw (B.H.M.).
† National Tsing Hua University.
‡ Academia Sinica.
§ Duke University.

10.1021/cg801423g CCC: $40.75
Published on Web 05/11/2009

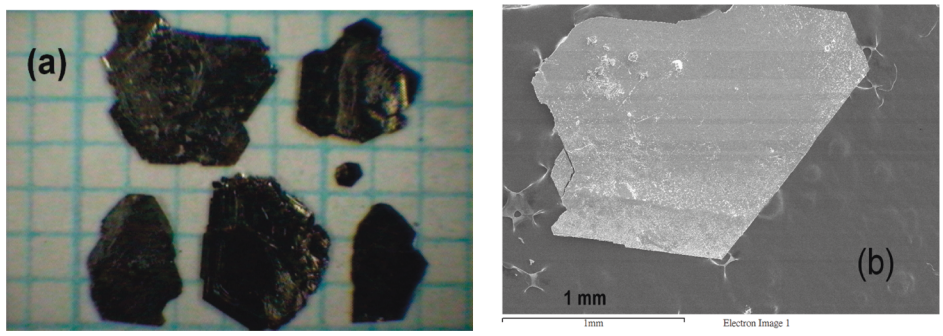

Figure 1. (a) Optical micrograph (background mesh size 1 mm) of $FeSe_{0.88}$ and (b) SEM micrographs of the and $FeSe_{0.85}$ crystals grown in KCl solutions (marker is 1 mm).

furnace and cut to recover the KCl crystalline mass with the FeSe crystals embedded in it. The KCl crystals were cut into smaller pieces to dissolve in water and recover the FeSe crystals. When the FeSe crystals separated, water was drained out; the crystals were rinsed 3−4 times in acetone to remove water and moisture sticking to the surface of the crystals. The rinsed crystals were dried in an oven at 80−90 °C before they were stored in evacuated desiccators and used subsequently for investigations. Washing the crystals in water did not produce any visible damage to the crystal surface even though slow attack could not be ruled out.

3. Results and Discussion

3.1. Crystal Morphology and Structure. Figure 1(a) and Figure 1(b) show the optical and SEM micrographs of the $FeSe_{0.88}$ crystals respectively. The optical micrograph shows small crystals that exhibit a smooth surface and sharp hexagonal plate like morphological features. Intergrowth is observed as the crystal size increases probably due to the inhomogeneous local supersaturation effects[17] as the solution was not stirred. The crystals measuring 2−3 mm across and 0.1−0.3 mm thick could be easily picked for measurements. Judging from the smooth faces on one side of the crystals, it appears that stable growth conditions were achieved. The second side shows growth spirals, which is typical of the bottom side of crystals grown from solutions. Even though crystals with other Se composition were also grown, we have chosen to report on $FeSe_{0.88}$ here to compare with the polycrystalline samples of $FeSe_{0.88}$ reported by Hsu et al.[7] The energy dispersive X-ray spectroscopic (EDS) analysis shows an average Fe/Se ratio of 46/54 in the $FeSe_{0.88}$ crystals and Fe/Se/Mn ratio of 41/52/7 (average of 5 measurements on different crystals), indicating a slight excess of Se. Less than 1 at % of K and Cl was observed in the crystals, indicating negligible flux inclusion. Oxygen was also observed in the EDS measurements, but the X-ray absorption near edge structures spectroscopy (XANES) measurements (not presented here) revealed only trace amounts as seen from the Fe, Fe−O like spectra. Besides, the Fe L-edge spectra that are sensitive to surface layers show higher oxygen compared to the Fe K-edge spectra that result from deeper layers of the crystal. Thus the presence of oxygen may be a result of cleaning the crystals with water following crystal growth as described earlier.

FeSe:Mn and $FeSe_x$ could also be grown from KBr solutions. Preliminary experiments show that the former did not exhibit superconductivity whereas the latter did when they were grown in KBr solutions. It is difficult to speculate the reason for this. It is likely that the superconducting α-FeSe phase is not easily stabilized in the presence of Mn in the KBr solution with a lower melting point (~730 °C) compared to KCl (~750 °C). Negligible flux inclusion was observed in the crystals grown from KBr solutions also.

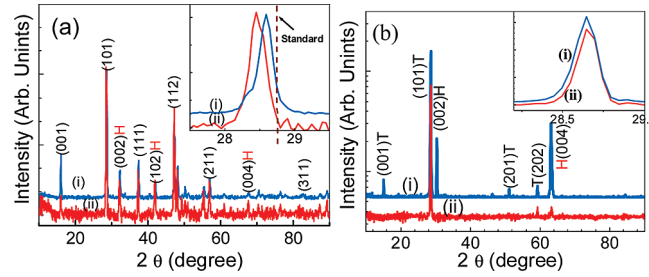

Figure 2. (a) Powder XRD patterns of (i) FeSe:$Mn_{0.1}$ and (ii) $FeSe_{0.88}$ crystals and (b) surface scans of the $FeSe_{0.85}$ crystal plates (i) without and (ii) with annealing (*y*-axis in log scale).

The powder XRD patterns recorded using crystals crushed into fine powder are shown in Figure 2(a). The pattern of $FeSe_{0.88}$ crystal appears to be similar to that reported by Hsu et al.[7] The patterns were fitted to the tetragonal space group *P*4/*nmm* of the α-FeSe phase and indexed. The lattice parameters obtained from fitting the patterns (for the $FeSe_{0.88}$) are a = 3.77163 Å; c = 5.52174 Å; α = β = γ = 90°; V = 78.54757 Å^3. These values are slightly higher than the values reported earlier.[7] One of the peaks marked H, belonging to the hexagonal β-phase only,[18] is observed in both patterns indicating the possible persistence of a small amount of β-phase in the crystals. It may be pointed out that some of the β-phase peaks overlap with the α-phase peaks. The presence of β-phase may be a result of the growth at high temperatures (>750) where the β-phase is more stable. For the sake of clarity, the strongest peak at 2θ = 28.5° is shown expanded in the inset of Figure 2(a). The main diffraction peaks in both crystals are found to shift slightly to a lower 2θ compared to the standard (for FeSe marked with dashed line) indicating an increase in the lattice parameters and a possible lattice distortion. The lattice distortion in the case of Mn doped crystal is slightly less compared to the $FeSe_{0.88}$ crystal. The influence of annealing the crystals *in situ* at 400 °C is shown in the XRD patterns of single crystal plates (that were available from later crystal growth runs) of $FeSe_{0.85}$ without (i) and with (ii) annealing given in Figure 2(b). A sharp and intense peak (101) at 2θ = 28.645°, a weak (202) reflection (at 59.345°) belonging to the α-FeSe phase and a weak reflection (004) reflection at 63.145° from the β-phase are seen in the pattern (ii) of the annealed crystal plates indicating a stabilization or transformation to the α-phase. On the other hand additional reflections (belonging to both phases) are seen in the pattern (i) of the crystal without annealing. The presence of the reflections corresponding to both the phases in the as grown crystal and their absence on annealing indicates that the two phases might coexist in the as grown crystals, probably forming a super lattice as in the case of doped alkali halides.[19] The

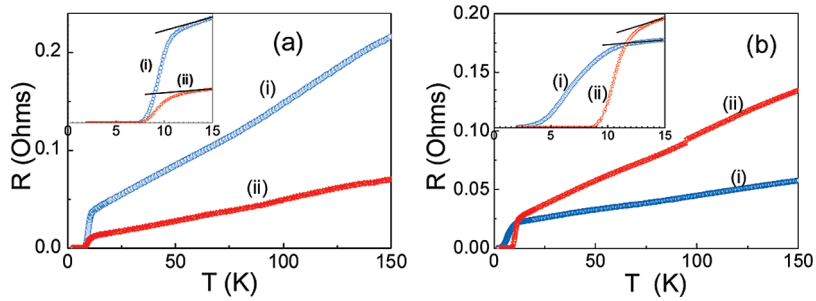

Figure 3. (a) R vs T plots of (i) $FeSe_{0.88}$ and (ii) $FeSe:Mn_{0.1}$ crystals and (b) $R-T$ plots of the $FeSe_{0.85}$ crystal (i) without and (ii) with the 400 °C annealing.

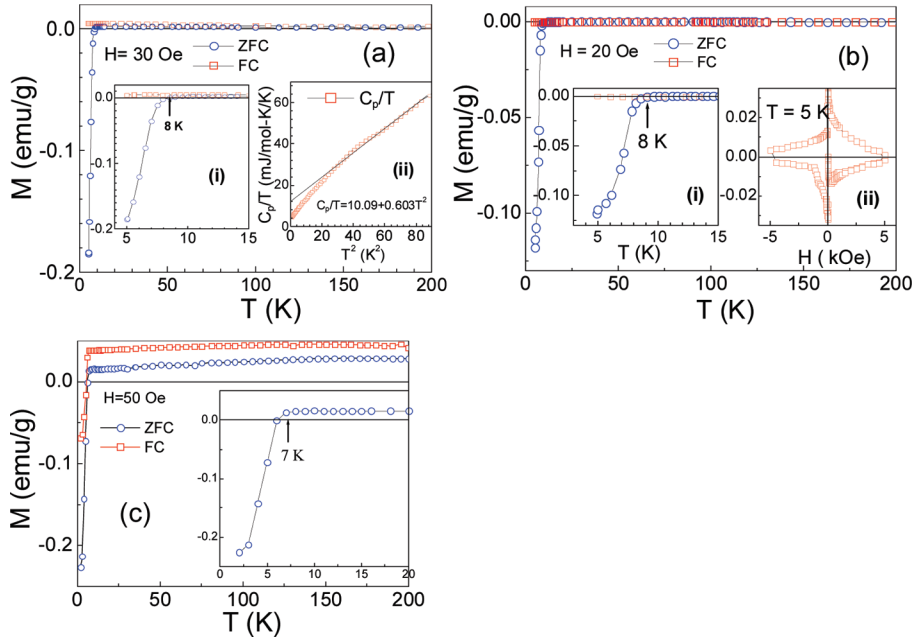

Figure 4. ZFC and FC M vs T curves for (a) $FeSe_{0.88}$ and (b) $FeSe:Mn_{0.1}$ crystals grown in KCl solution and (c) $FeSe_{0.85}$ crystal grown in KBr solution. All crystals were annealed *in situ* at 400 °C for 24 h while cooling to room temperature.

expanded view of the 28° peak does not show any shift indicating that annealing does not influence the crystal structure.

3.2. Transport Measurements. Resistance (R) vs temperature (T) plots of $FeSe_{0.88}$ and $FeSeMn_{0.1}$ grown under identical conditions are shown in Figure 3(a). The curves for $FeSe_{0.88}$ exhibit metallic behavior in the normal state and show zero resistance at 7.5 K following a broad transition from 11 K (shown by the fitting in the inset) similar to the bulk.[7] The Mn doped crystal shows similar characteristics. $R-T$ plots of the $FeSe_{0.85}$ crystals grown with and without 400 °C annealing are shown in Figure 3(b). The transition is seen to be sharper in the annealed crystals with zero resistance at 8.5 and onset at 13 K while these are observed at 2.5 and 11.5 K respectively in the crystals without annealing.

3.3. Magnetic Measurements. Figure 4 shows the zero field cooled (ZFC) and field cooled (FC) magnetization (M) vs temperature (T) curves for (a) $FeSe_{0.88}$ and (b) $FeSe:Mn_{0.1}$ (grown in KCl) and (c) $FeSe_{0.85}$ (KBr grown) crystals. The crystals were oriented with the (101) plane perpendicular to the magnetic field. The curves are similar to those of the bulk samples reported earlier[7] but show lesser Pauli susceptibility in both the ZFC and FC curves in the normal state indicating low background magnetic (Fe and others) impurity content, expected since impurities are rejected at solid−liquid interface during crystal growth. The anomaly in the susceptibility at ∼105 K reported in bulk samples[7] was found to be much smaller in the crystals probably due to the orientation of the crystals. A sharp superconducting transition is observed at 8 K as in the bulk, in both the Se deficient and Mn doped crystals. The $M-H$ curves obtained on these crystals (inset (ii) Figure 4(b)) confirm the superconductivity in these crystals. The specific heat $(C_p)/T$ vs T^2 plots recorded on $FeSe_{0.85}$ crystals shown in the inset (ii) of Figure 4(a) shows a small specific heat jump at 7.5 K corresponding to the superconducting transition indicative of bulk superconductivity. A fitting of the curve in the normal state yields a γ value of 10.09 mJ/mol-K^2 and a slope 0.603 which are very close to those reported on the bulk. The superconducting fraction calculated from Figure 4(a) which is corrected for the demagnetization factor is ∼35−40%. The crystals crushed into powder yield a value of 11%. This big difference is expected as the powder might also undergo chemical changes during handling that may be detrimental to the superconductivity aside from a lack of compacting. It was also observed that the crystals exhibit orientation dependence (not shown here) in the magnetic properties similar to the YBCO type superconductors indicating that they may not represent conventional superconductors as concluded by Hsu et al.[6] ZFC and FC M vs T curves for the $FeSe_{0.85}$ crystal grown from KBr solutions are given in Figure 4(c). It is seen that

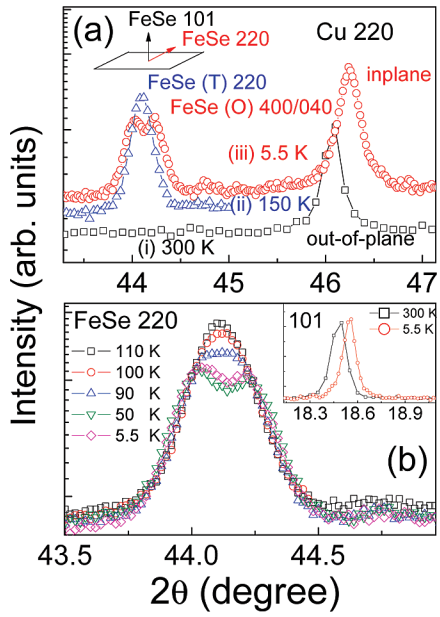

Figure 5. (a) The (220) Bragg diffraction peaks of FeSe single crystal and polycrystalline copper holder at 300 K (i), 150 K (ii) and 5.5 K (iii). The orientation of the crystal with respect to the incident X-ray beam is indicated with arrows in the figure. The FeSe (220) peak is not seen in the out-of-plane measurement indicating good crystallinity of FeSe; (b) the temperature dependence of the FeSe (220)(T) (in-plane) splitting to FeSe (O) (400) and (040) reflections at temperature around 90−100 K. The inset shows the FeSe (101) out-of-plane measurement at 5.5 K and 300 K.

the Pauli susceptibility is somewhat larger compared to the KCl grown crystals but nearly unchanged with temperature. The transition is observed at 7 K, which is slightly lower than 8 K observed in the KCl grown crystals.

3.4. Temperature Dependent X-ray Scattering Measurements. Figure 5 shows the 4-circle X-ray scattering data obtained at different temperatures that were collected using synchrotron source (BL12b2 at SPring 8) with incident beam of wavelength 0.1 nm. A mosaic of several small crystals was used in this experiment to provide larger area needed for obtaining sufficient intensity of the signal. Figure 5(a) (i) shows the pattern obtained with the (101) plane of the FeSe crystal oriented out-of-plane with the incident X-ray beam. The pattern shows only the (220) reflection of the polycrystalline Cu sample holder confirming good crystallinity of the FeSe sample. The patterns obtained with the crystals oriented in-plane with the incident beam and measured at 150 and 5.5 K are presented in Figure 5(a) (ii) and (iii) respectively that show a temperature dependent phase transition similar to that observed in the bulk samples.[7] The splitting of the Bragg peak of FeSe (220) to FeSe orthorhombic (400) and (040) is observed at 5.5 K. However, due to the mosaic of crystals used for the measurements, the in-plane pattern shows two Bragg peaks that correspond to two *d*-spacings of FeSe orthorhombic (400) and (040) instead of only (400). In contrast to this the tetragonal phase (101)T peak at 300 K shifts to a higher θ at 5.5 K indicating the orthorhombic distortion as shown in the inset of Figure 5(b). Similar splitting was also observed with the Bragg peaks (221) and (311). More detailed temperature dependence of the scattering is presented in the patterns of Figure 5(b) showing the changes to the (200)T peak and the appearance of the (400)O peak. It is worth mentioning that the phase transition temperature of α-FeSe from tetragonal (*P*4/*nmm*) at room temperature to orthorhombic (CMMA) symmetry occurs around 100 K similar to that observed in case of the bulk. This phase transition around 100 K is reflected as a weak anomaly in the $R-T$ and $M-T$ curves presented above and thus supports the conclusions drawn by Hsu et al.,[7] namely, the possibility that this is an unusual superconductor. Unlike the bulk, where a much stronger anomaly was observed in the resistivity and susceptibility measurements at ∼105 K, the crystals show a weak feature probably due to the orientation of the crystal as mentioned above. Such phase transition is generally associated with spin wave magnetic order pointing to the possibility that FeSe is somewhat different from traditional superconductors.

Small hexagonal cylindrical crystals were also observed among the hexagonal α-FeSe plate crystals. It was found from the XRD analysis that these represent predominantly the β-FeSe phase and also did not show superconductivity. From the small size of the crystals, it appears that these grew during the final stages of growth, namely, at a lower temperature.

Annealing the crystals at 400 °C *in situ* during the cooling program appears to be beneficial to the properties of the Se deficient crystals, but it kills superconductivity in the Mn doped crystals. While $FeSe_{0.85}$ crystals grown in KBr solutions show a predominant α-phase and superconductivity as shown in Figure 3(c), the Mn doped crystals show predominant β-phase and no superconductivity (not shown here). Thus it is appears that Mn doped crystals are better grown from KCl solutions and the Se deficient ones from KBr. More work is needed to establish a definitive conclusion about the choice of a better solvent for FeSe crystal growth and also the influence of crystal growth temperature and annealing conditions. However, judging from the rates of growth it appears that KCl could be used as a good solvent to grow large crystals of FeSe.

4. Conclusion

In conclusion, crystals of Se deficient and doped FeSe were grown from KCl solutions that exhibit similar superconducting properties as those of the bulk. The crystals represent a predominantly α-FeSe phase with a small β-FeSe phase under normal growth conditions. Annealing *in situ* during cooling for ∼15−24 h at 400 °C appears to stabilize the α-phase and increases the zero resistance temperature to 8.5 K. The influence of proper annealing conditions on the stabilization of the α-phase and the physical properties needs further investigation.

Acknowledgment. This work was supported under National Science Council (NSC) of the Republic of China Grant No. NSC-96-2112-M-001-026-MY3. One of the authors (S.M.R.) is grateful to the NSC for financial support, and B.H.M. is grateful for the financial support from Academia Sinica. We thank the National Synchrotron Search Centre, Taiwan, for experimental support in this work.

Supporting Information Available: This material is available free of charge via the Internet at http://pubs.acs.org.

References

(1) Jain, B. K.; Singh, A. K.; Chandra, K. *J. Phys. F: Met. Phys.* **1978**, *8*, 2625, and references therein.
(2) Hirakawa, K. *J. Phys. Soc. Jpn.* **1957**, *12*, 929.
(3) Schuster, W.; Mikler, H.; Komarek, K. L. Transition metal-Chalcogen systems, VII: the Iron-Selenium Phase Diagram (in English). *Monatsh. Chem.* **1979**, *110*, 1153.
(4) Okomoto, H. *J. Phase Equilib.* **1991**, *12*, 383, and references therein.

(5) Feng, Q. J.; Shen, D. Z.; Zhang, J. Y.; Li, B. S.; Li, B. H.; Lu, Y. M.; Fan, X. W.; Liang, H. W. *Appl. Phys. Lett.* **2006**, *88*, 012505.
(6) Wu, X. J.; Zhang, Z. Z.; Zhang, Y. J.; Ju, Z. G.; Shen, D. Z.; Li, B. H.; Shan, C. X.; Lu, Y. M. *J. Cryst. Growth* **2007**, *300*, 483.
(7) Hsu, F. C.; Luo, J. Y.; Yeh, K. W.; Chen, T. K.; Huang, T. W.; Wu, P. M.; Lee, Y. C.; Huang, Y. L.; Chu, Y. Y.; Yan, D. C.; Wu, M. K. *Proc. Natl. Acad. Sci. U.S.A.* **2008**, *105*, 14262.
(8) Kamihara, Y.; Watanabe, T.; Hirano, M.; Hosono, H. *J. Am. Chem. Soc.* **2008**, *130*, 3296.
(9) Takahashi, H.; Igawa, K.; Arii, K.; Kamihara, Y.; Hirano, M.; Hosono, H. *Nature* **2008**, *453*, 376.
(10) Zhang, S. B.; Sun, Y. P.; Zhu, X. D.; Zhu, X, B.; Wang, B. S.; Li, G.; Lei, H. C.; Luo, X.; Yang, Z. R.; Song, W. H.; Dai, J. M. *Supercond. Sci. Technol.* **2009**, *22*, 015020.
(11) Subedi, A.; Zhang, L.; Singh, D. J.; Du, M. H. *Phys. Rev.* **2008**, *78*, 134514.
(12) Mizuguchi, Y.; Tomioka, F.; Tsuda, S.; Yamaguchi, T.; Takano, Y. *Appl. Phys. Lett.* **2008**, *93*, 152505.
(13) Xu, C.; Sachdev, S. *Nat. Phys.* **2008**, *4*, 898.
(14) Yeh, K. W.; Huang, T. W.; Huang, Y. L.; Chen, T. K.; Hsu, F. C.; Wu, P. M.; Lee, Y. C.; Chu, Y. Y.; Chen, C. L.; Luo, J. Y.; Yan, D. C.; Wu, M. K. *Europhys. Lett.* **2008**, *84*, 37002.
(15) Li, Y.-F.; Zhu, L.-F.; Guo, S.-D.; Xu, Y.-C.; Liu, B.-G. *J. Phys.: Condens. Matter* **2009**, *21*, 115701.
(16) Mazin, I. I.; Johannes, M. D. *Nat. Phys.* **2009**, *5*, 141.
(17) Elwell, D.; Scheel, H. J. In *Crystal Growth from High Temperature Solutions*; Academic Press: New York, 1975.
(18) Alsen, N. *Geol. Foeren. Stockholm Foerh.* **1925**, *47*, 19.
(19) Lilley, E.; Newkirk, J. B. *J. Mater. Sci.* **1967**, *2*, 567.

CG801423G